Asian Journal of Chemistry Vol. 21, No. 7 (2009), 5363-5372

In Silico Screening and ADME Predictions of Some Quinazolinones as Potential Dihydrofolate Reductase Inhibitors for Anticancer Activity

A.G. NERKAR*, S.A. GHONE and A.K. THAKER
Department of Pharmaceutical and Medicinal Chemistry, School of Pharmacy and Technology Management, SVKM's NMIMS University, Mumbai-400 056, India
E-mail: agn971981@yahoo.co.in

In this paper, *in silico* screening, conducted before the actual synthesis of some 'best fit' quinazolinone moieties as the possible inhibitors of dihydrofolate reductase enzyme for anticancer activity is reported. Molecular docking of a set of ligands from series of 6,6'-methylene-*bis*-2-methyl-3-((2/3-aryl)heterocycyl-3/4/5-one)quinazolin-4-(3*H*)-one (**BQ**$_{1\text{-}132}$), 2-alkyl/phenyl-3-(2/3-aryl heterocycyl-3/4/5-one)quinazolin-4(3*H*)-one (**QHIP**$_{1\text{-}132}$, **QHP**$_{1\text{-}132}$, **QHM**$_{1\text{-}132}$), 2-phenyl-3-(arylideneamino)-quinazolin-4(3*H*)-one (**QSB**$_{1\text{-}31}$) was performed using Glide® as the docking module. The prediction of absorption, distribution, metabolism and excretion (ADME) properties was obtained with the QikProp® 2.5 module. The 3D ligand-protein complex structure of human dihydrofolate reductase (**1BOZ**) was obtained from the Protein Database Bank (RCSB PDB) and processed for the docking using the protein preparation wizard module. Methotrexate (MTX) a potent inhibitor of dihydrofolate reductase enzyme was included in test sets, to compare the Glide score (G score) of designed analogues. The binding affinities of different ligands were compared to give E-model score values. Analogues showed comparative G scores with MTX and Raltitrexed.

Key Words: *In silico* screening, Quinazolinones, Docking, Anticancer activity.

INTRODUCTION

The computer aided drug designing involves various strategies; one of it being the structure based drug design that analyses the binding site of the target protein, in its complex with the ligand. It also involves docking wherein the substrates or the ligands and their low energy conformations for the proteins are made to fit their active site with the help of the drug design software. Docking methods have a great advantage as compared to 2D similarity and 3D pharmacophore search methods as it utilizes 3D receptor structure in a quantitative way[1]. Docking calculations alone or combined with the virtual screening has been carried out to develop the dihydrofolate reductase and tyrosine kinase inhibitors[2], agonists and antagonists of A3 adenosine receptors[3], acetylcholine esterase inhibitors[4], glycogen phosphorylase inhibitors[5],

thymidyalte synthase inhibitors[6], glutathione and trypanothione reductase inhibitors[7], COX-1 inibitors[8], *etc*.

Dihydrofolate reductase (E.C.1.5.1.3) is the most studied enzyme for the drug designing of anticancer agents. Dihydrofolate reductase functions as the catalyst for the reduction of the dihydrofolate to tetrahydrofolate that generates reduced folate carriers of one carbon fragments and is the important co-factor in the biosynthesis of nucleic acids and amino acids. The inhibition dihydrofolate reductase leads to the partial depletion of intracellular reduced folates with the subsequent limitation of cell growth[9]. Thus inhibitors of this enzyme are potential anticancer agents as dihydrofolate reductase plays important role in the S-Phase of cell cycle. Recognition of MTX, chemically a pterin analogue, as an inhibitor of the dihydrofolate reductase attracted the attention towards the development of folate antagonists as anticancer agents[10]. MTX is a potent inhibitor of dihydrofolate reductase, as a consequence of dihydrofolate reductase inhibition, intracellular levels of tetrahydrofolate coenzymes are decreased, resulting in inhibition of thymidylate synthase and consequently DNA and purine biosynthesis[11]. Literature reveals that the quinazoline moiety has the potential for the dihydrofolate reductase inhibition and several 2,4- diaminoquinazoline analogues were evaluated for the dihydrofolate reductase inhibition and found potent as compared with MTX[12-19].

EXPERIMENTAL

Molecular modeling: The computation was carried out in Schrodinger molecular modeling software. Molecular docking was performed for quinazolinones analogues using the GLIDE® integrated Maestro® 7.5 interface on the Linux operation system. The molecules were subjected to predict the ADME properties using the QikProp® 2.5 module. ChemOffice 6.0 software was used to draw the 3-D structures and for the conversion of the structure to mol files.

Selection of the protein file: For the docking purpose the PDB file 1BOZ was selected after evaluating several files from the protein database bank www.rcsb.org. 1. The file contains the 3-D crystalline structure of DHFR from Human origin. 2. Further the enzyme file was subjected to structure validation procedures.

Structure validation of the enzyme: The errata report and the Ramachandran plot was obtained from the NIH MBI sever for evaluation of protein structures and are given in Figs. 1 and 3, respectively. The structure was also validated using mol probidity Ramachandran (Fig. 2).

Designing of the molecules and library design: A set of analogues of series 6,6'-methylene-*bis*-2-methyl-3-((2/3-aryl)heterocycyl-3/4/5-one)quinazolin-4-(3*H*)-one (**BQ**$_{1\text{-}132}$), 2-alkyl/phenyl-3-(2/3-aryl heterocycyl-3/4/5-one)quinazolin-4(3*H*)-one (**QHIP**$_{1\text{-}132}$, **QHP**$_{1\text{-}132}$, **QHM**$_{1\text{-}132}$) and 2-phenyl-3-(arylideneamino)quinazolin-4(3*H*)-one (**QSB**$_{1\text{-}31}$) shown in Fig. 5 were designed based upon their feasibility of synthesis and possible positional substitutions. MTX a known inhibitor of human dihydrofolate reductase was included in the ligand sets. This total constituted around 1000 molecules.

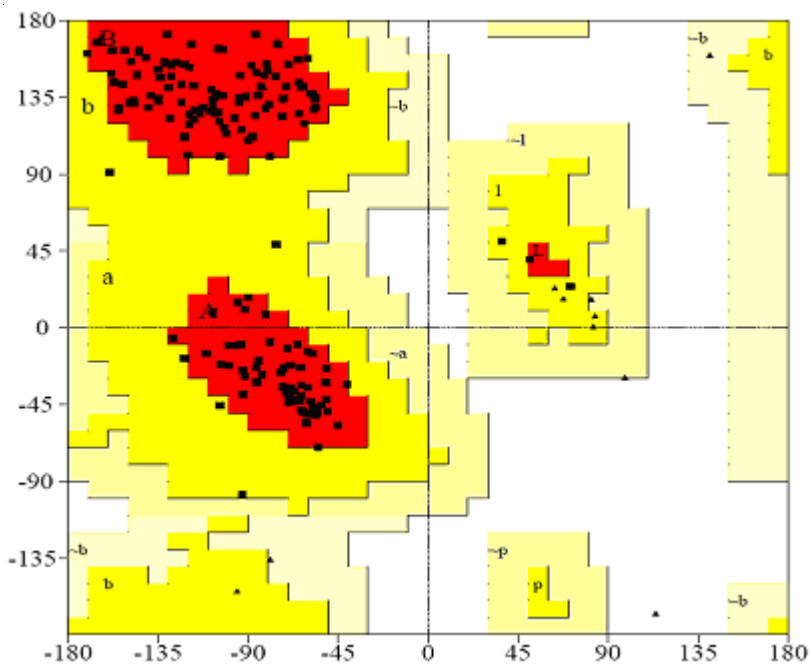

Fig. 1. Ramachandran plot of the PDB ID 1BOZ

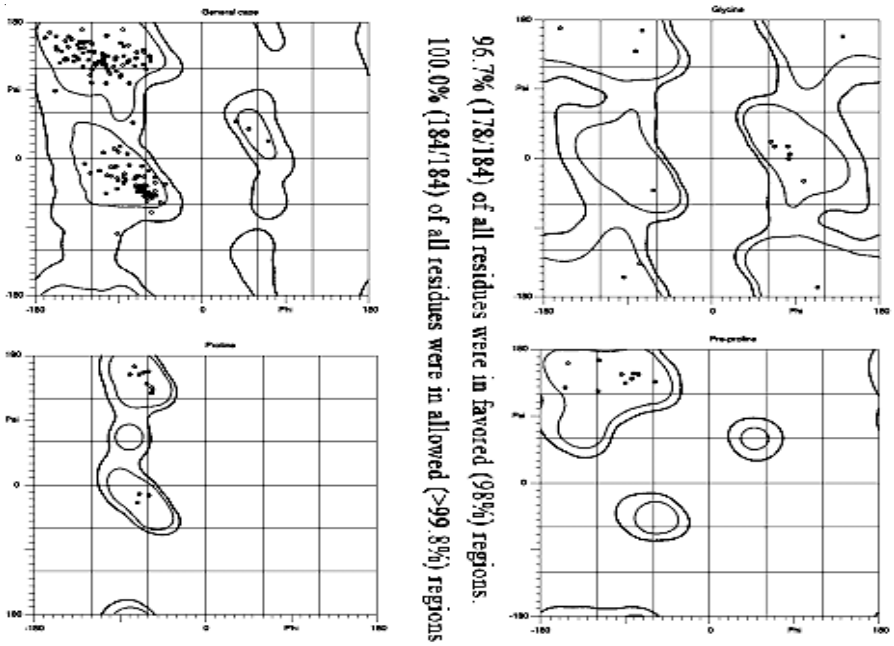

Fig. 2. Mol probidity Ramachandran plot

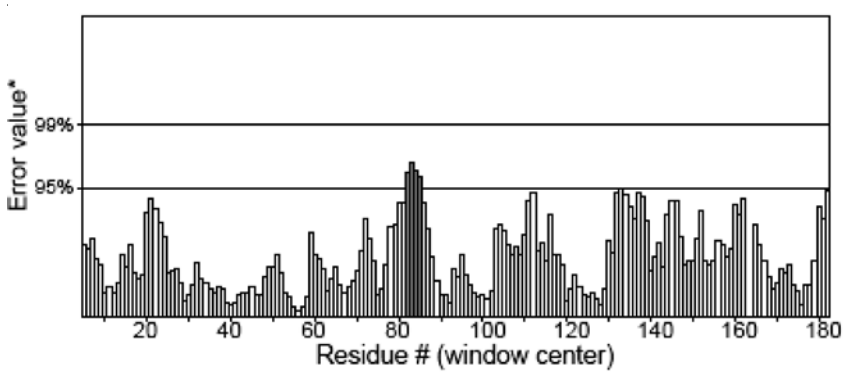

Overall quality factor: 97.27 %

Fig. 3. Errata report of the PDB ID1BOZ

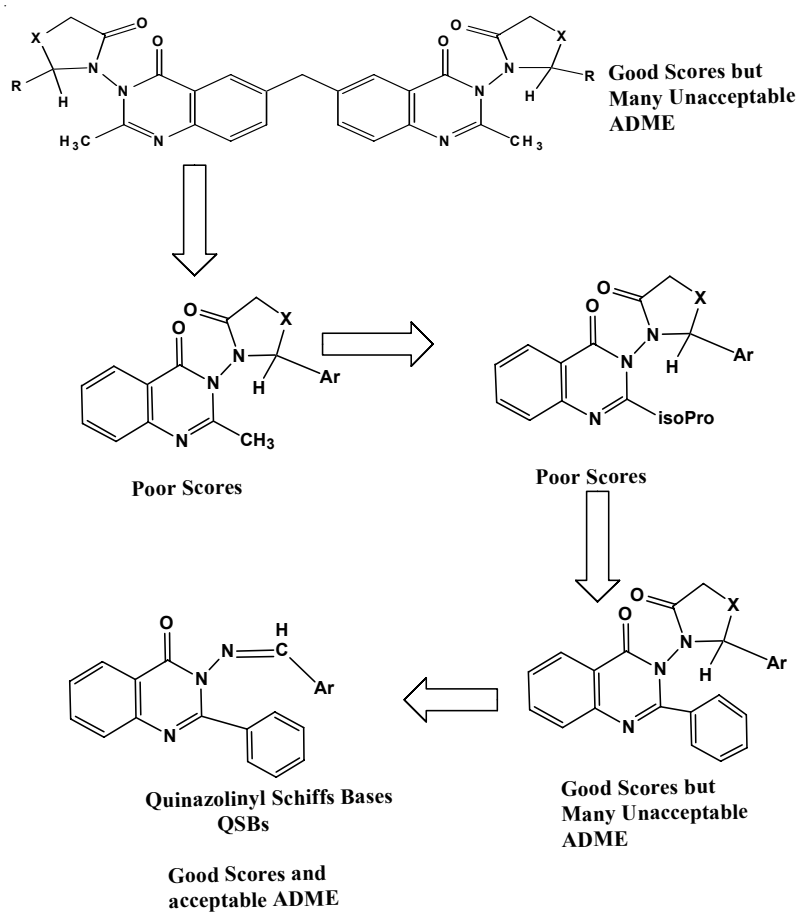

Fig. 4. Flow chart of virtual screening for emergence of acceptable molecules with good inhibition scores on DHFR enzyme. The azetidinyl derivatives are not shown.

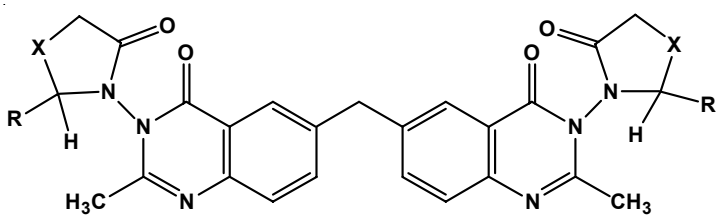

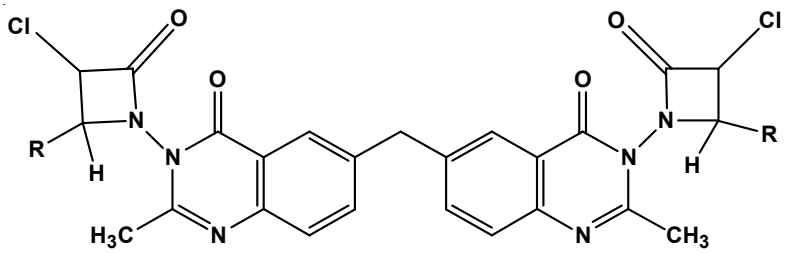

$BQ_{1\text{-}132}$ series

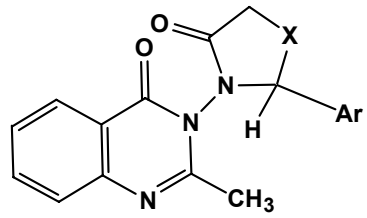

$QHM_{1\text{-}132}$

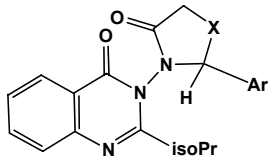

$QHIP_{1\text{-}132}$

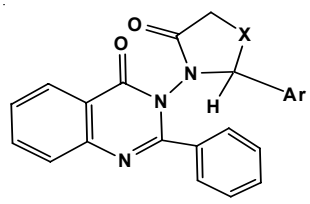

$QHP_{1\text{-}132}$

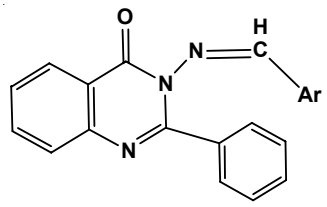

$QSB_{1\text{-}31}$

X = NH, S, O

R=Ar = C_6H_5, 4-OH-C_6H_4, 4-Cl-C_6H_4, 4-NO_2-C_6H_4, 4-(*iso*C_3H_7)-C_6H_4, 4-F-C_6H_4, 4-Br-C_6H_4, 4-(OCH_3)-C_6H_4, 3-OH-4-(OCH_3)-C_6H_4, 3,4-(OCH_3)$_2$-C_6H_3, 3,4-(OH)$_2$-C_6H_3, 3-(OCH_3)-C_6H_4, 3-NO_2-C_6H_4, 3-OH-C_6H_4, 3-Br-C_6H_4, 3-Cl-C_6H_4, 2-OH-3-(OCH_3)-C_6H_3, 2-OH-4-(OCH_3)-C_6H_3, 2,5-(OCH_3)2-C_6H_3, 2,4-(OCH_3)$_2$-C_6H_3, 2,4-(Cl)$_2$-C_6H_3, 2,6-(Cl)$_2$-C_6H_3, 2,5-(OH)$_2$-C_6H_3, 2,4-(OH)$_2$-C_6H_3, 2,3-(OCH_3)$_2$-C_6H_3, 2-Furano, 2-Thiophene, 2-(OCH_3)-C_6H_4, 2-Br-C_6H_4, 2-NO_2-C_6H_4, 2-Cl-C_6H_4

Fig. 5. Structures of the ligands

TABLE-1
SCORES OF 2 BEST FIT LIGANDS FROM THE SERIES OF BQ_{1-132}, $QHIP_{1-132}$, QHP_{1-132}, QHM_{1-132} SERIES

Code name	Ar	X	G-Score	E-Score	ΔG^*_{Energy}	H-Bonds
BQ_{94}	3-Cl-C_6H_4	NH	-9.40	-101	-63.1	2
BQ_{95}	2-Cl-C_6H_4	NH	-9.36	-90.5	-58.3	2
BQ_{35}	4-Br-C_6H_4	O	-9.02	-94.6	-59.6	1
BQ_{58}	Pyrollidinyl	O	-9.00	-94.7	-59.8	2
BQ_{13}	3-OH-C_6H_4	S	-9.51	-101.7	-61.0	1
BQ_{27}	Pyrollidinyl	S	-8.94	-98.0	-61.8	3
BQ_{64}	2-Cl-C_6H_4	Azetidinyl	-9.12	-101.5	-63.8	1
BQ_{83}	Furfuryl	Azetidinyl	-9.06	-93.0	-63.0	1
$QHIP_{124}$	Naphthanyl	NH	-8.64	-69.0	-49.8	1
$QHIP_{114}$	Furfuryl	NH	-8.09	-58.3	-40.5	2
$QHIP_{44}$	3-OH-C_6H_4	O	-7.87	-63.2	-40.7	2
$QHIP_{45}$	4-OH-C_6H_4	O	-7.85	-140.8	-53.6	6
QHM_{15}	C_6H_5	NH	-6.50	-102.3	-104.5	1
QHM_{17}	2,5-$(OCH_3)_2$-Ph-	NH	-5.50	-96.3	-103.5	1
QHM_{92}	4-NO_2-C_6H_4	O	NG	NG	NG	NG
QHM_{65}	4-Cl-C_6H_4	O	NG	NG	NG	NG
QHM_{37}	3-Cl-C_6H_4	S	NG	NG	NG	NG
QHM_{19}	2,5-$(OH)_2$-Ph-	S	NG	NG	NG	NG
QHM_{13}	3,4-$(OH)_2$-Ph-	Azetidinyl	-8.31	-79.8	-49.7	1
QHP_{107}	4-OH-C_6H_4	NH	-7.80	-73.4	-47.0	1
QHP_{109}	2,5-$(OCH_3)_2$-Ph-	NH	-7.80	-73.4	-47.9	1
QHP_{43}	3,4-$(OH)_2$-Ph-	O	-8.03	-68.2	-44.7	1
QHP_{54}	2-OH-4-OCH_3-Ph	O	-8.09	-58.3	-40.5	2
QHP_{19}	3,4-$(OH)_2$-Ph-	S	-8.92	-83.1	-49.3	2
QHP_{13}	3-OH-C_6H_4	S	-8.61	-79.8	-49.7	1
QHP_{28}	2-NO_2-C_6H_4	Azetidinyl	-8.59	-70.5	-42.9	3
QHP_{70}	3-OCH_3-C_6H_4	Azetidinyl	-8.02	-74.4	-49.3	3
QSB_{15}	2,6-$(Cl)_2$-C_6H_4	-	-11.0	-173.0	-76.6	2
QSB_{23}	4-Cl-C_6H_4	-	-10.10	-172.0	-78.6	2
QSB_{33}	2-OH-4-OCH_3-Ph	-	-9.80	-162.0	-48.3	2
QSB_3	C_6H_4	-	-9.70	-148.8	-50.0	2
QSB_{21}	Furfuryl	-	-9.50	-145.8	-50.5	2
MTX	-	-	-10.10	-163.3	-63.6	8
RTX	-	-	-10.10	-163.3	-63.6	8

Number of H-bondings with the DFHR enzyme; *Expressed as Kcal/mol
NG = No good posses found

Docking of the molecules: The ligands were prepared by LigPrep[20] module which produces a single low-energy 3D structure with correct chiralities for each successfully processed input structure. LigPrep[20] also produces a number of structures from each input structure with various ionization states, tautomers, stereochemistry, ring conformations and eliminates molecules using various criteria including molecular weight or specified numbers and type of functional groups present, based upon the OPLS-2005 Molecular mechanics force field.

TABLE-2
QikProp ADME PREDICTIONS OF GOOD SCORING ANALOGUES

Code name	Stars	P*	HERG*	Caco	BB*	Khsa*	LROF[+]	NOM[$]	%HA[@]
BQ_{94}	4	1.010	-8.202	0.171	-3.197	0.290	2	11	43.00
BQ_{95}	4	3.399	-8.153	11.855	-0.446	0.640	2	4	42.00
BQ_{35}	5	1.071	-8.261	0.195	-3.129	0.292	2	12	56.00
BQ_{58}	5	3.413	-8.437	13.840	-0.462	0.655	2	13	37.00
BQ_{13}	9	2.444	-8.047	12.048	-0.876	0.344	2	10	43.00
BQ_{27}	9	4.236	-8.180	13.514	-0.214	0.831	2	9	51.00
BQ_{64}	3	1.126	-8.124	1.202	-2.0417	0.228	2	11	54.00
BQ_{83}	3	1.085	-8.080	1.108	-2.076	0.226	2	11	55.00
$QHIP_{124}$	6	1.842	-7.677	13.787	-0.864	-0.053	2	11	59.00
$QHIP_{114}$	6	-0.185	-7.893	0.160	-3.257	-0.045	2	13	57.00
$QHIP_{44}$	3	2.889	-8.093	11.855	-0.520	0.505	2	13	53.00
$QHIP_{45}$	7	1.501	-7.972	2.938	-1.798	0.167	2	10	61.00
QHM_{15}	6	1.316	-7.760	2.224	-1.883	0.146	2	12	69.00
QHM_{17}	8	4.172	-8.053	11.855	-1.000	1.132	2	10	73.00
QHM_{92}	3	1.872	-8.483	7.373	-1.059	0.379	2	9	47.00
QHM_{65}	9	1.071	-8.261	0.195	-3.129	0.292	2	9	45.00
QHM_{37}	9	1.010	-8.202	0.171	-3.197	0.290	2	9	41.00
QHM_{19}	3	2.720	-67.300	0.039	-2.520	0.003	2	15	47.00
QHM_{13}	5	4.140	-6.180	0.045	-0.900	-0.040	2	11	57.35
QHP_{107}	5	2.930	-7.130	0.572	-1.720	0.200	2	11	81.51
QHP_{109}	6	2.760	-6.580	0.684	-2.950	0.310	2	13	76.00
QHP_{43}	5	4.052	-6.830	0.329	-1.140	0.550	2	13	43.85
QHP_{54}	3	4.610	-6.950	0.431	-0.670	0.760	2	9	70.81
QHP_{19}	7	6.880	-7.380	0.532	-1.180	1.200	2	7	82.80
QHP_{13}	2	3.600	-5.480	0.326	-3.250	-0.080	2	12	89.38
QHP_{28}	0	1.180	-7.890	176	-3.370	-0.080	0	2	69.37
QHP_{70}	0	1.070	-8.260	180	-3.120	-0.450	0	2	90.00
QSB_{15}	0	1.570	-8.000	185	1.240	-2.920	0	2	95.00
QSB_{23}	0	1.320	-5.320	290	1.270	-0.080	0	2	93.00
QSB_{33}	0	1.690	-4.320	297	-1.870	-0.234	0	2	100.00
QSB_{3}	0	1.740	-3.280	325	-1.530	-4.120	0	2	94.00
QSB_{21}	0	1.580	-2.170	182	-1.700	-2.120	0	2	92.00

[+]Lipinski's rule of five, [$]Number of metabolites, @% percentage of human oral absorption

Energy minimization of the protein: The crystal structure of the human dihydrofolate reductase enzyme (1BOZ) was obtained from the protein data bank (RCSB PDB) and contains the chain A of the enzyme complexed with the known inhibitor. This chain A was selected for the docking studies. The protein preparation wizard was used for the protein preparation that runs in two steps. In step one, protein assignment is carried out wherein the bond geometries and the order of the bonds of the protein molecule are optimized followed by impref minimization in which, the energy minimization is carried out at the default cut off RMSD value of 0.30 Å, as the second step.

Receptor grid preparation: The coordinates of human dihydrofolate reductase chain A were obtained from the crystal structure of the protein file 1BOZ (processed file from the protein preparation wizard). The van der Waals radii were scaled up by the default value of 1.00 Å for the atoms with the partial charges of less than 0.25. The receptor grid was generated around the centroid of the ligand contained by PDB file and the ligands with cut off size of 10 Å were allowed to dock. Hydrophobic, hydrogen bonding/ metal bonding and positional constraints were not included for the screening purpose in the settings.

Docking of the ligands: Docking was carried out using the Glide module of software which uses the suite of hierarchical filters to remove unlikely solutions starting from low level approximation (distance matches) to high level calculations (force field based MCSA minimization) with free energy scoring. Glide implements a novel algorithm for rapid conformational generation minimizing computational costs by clustering the core regions of the generated 3D conformations and treating the positions of rotamer groups at the end essentially independently[21]. Further, virtual screening through hierarchical docking filters allows a systematic search of all possible ligand conformations, positions and orientations. The ligands were docked flexibly to write up to 10000 poses per ligand in the extra precision mode. This produced result of docking of the ligands having the G-Scores and E-model Scores.

Validation of the docking protocol: Validation of the docking protocol was carried by pose regeneration of the ligand structure as seen in the crystallized PDB and overlapping the best dock pose of the ligand and the as it is obtained PDB, also validation of the docking protocol was carried out as reported by Vijullatha *et al.*[22] with correlation coefficient r^2 of 0.9303.

ADME Predictions of the best fit molecules: The ligands with the comparable scores with MTX were subjected to predict absorption, distribution, metabolism and excretion properties using the QikProp module of the software. QikProp settings determine which molecules are flagged as being dissimilar to other 95 % of the known drugs. Here the predicted significant ADME properties such as water octanol partition coefficient (QP log P), predicted number of metabolites (NOM), predicted solubility (QP log S), predicted IC_{50} value for blockage of HERG K^+ channels (QP log HERG), predicted gut-blood barrier (QPPCaco), predicted blood brain barrier partition coefficient (QP log BB), predicted binding to the serum albumin (QP log Khsa), predicted percentage human oral absorption (% HA) and violations of the Lipinski's rule of five (LROF). The number of stars indicate the deviations from the 95 % of the known drugs. However, the stars are for the violations taking overall properties into consideration. Besides these predictions the software also predicts the number of amides, number of amidines CNS activity, total solvent accessible surface area (SASA), hydrophobic and hydrophilic component of SASA (FOSA and FISA), weakly polar component of SASA (WPSA), dipole moment, number of donors and acceptable hydrogens, *etc.*[23].

RESULTS AND DISCUSSION

From Figs. 1-3 the protein structure was validated and found with 97.27 % quality. In an order to arrive best fit molecules with acceptable ADME properties, a compound library of around 1000 molecules was generated and screened prior to actual synthesis to arrive at better molecules best fit in the receptor binding pocket.

Substantial changes in the substituent positions were carried out *viz.* from *bis* molecules, to the change such as 2-isopropyl, methyl and phenyl. Alkyl/phenyl substitutions at 2 positions on quinazolinone ring results in increased anticancer activity and it was found that phenyl at 2 positions of Schiff's bases imparts molecules better G-score and E-model score. Moreover all the molecules were found to be fitting the actual binding pocket of the molecules as seen with MTX. MTX has the ten inter hydrogen bondings with the receptor namely Thr-56 interacting with O-22 of the ligand atom, Ser-118 (OH) with O-22, Ser-118 (NH) with O-22, Gly-117 with O-31, Lys-55 with O-58, Thr-56 with O-58 Ser-119 (OH) with O-59, Ser-119 (NH) with O-59, Val-115 with H-40 and Ser-59 with H-60. MTX showed ΔG binding energy of -163.0 K/cal and the QSB series did show better value than this proving that MTX is the potent inhibitor of human DHFR. Thus it can be concluded that these amino acid residues contribute towards the active binding sites of the DHFR enzyme for interactions with MTX in the chain A of the enzyme and the interactions with these residues are taken standard for predicting the interactions with other ligands. Most of the good scoring ligands from the series $QSB_{1\text{-}31}$ were found to interact with atleast one of the same amino acid residues as seen in case of MTX. Thus, it can be concluded that $QSB_{1\text{-}31}$ series were found with better ADME properties and can serve as potential molecules as anticancer agents.

ACKNOWLEDGEMENTS

The author AGN is highly obliged with Prof. Dr. R. S. Gaud, Dean and Prof. Dr. Krishnapriya Mohanraj of School of Pharmacy and Technology Management for their incredible support and guidance.

REFERENCES

1. A.K. Chakraborty and R. Thilagavathi, *Internet Electron. J. Mol. Des.*, **3**, 704 (2004).
2. A. Gangjee, Y. Zeng, M. Ihnat, L.A. Warnke, D.W. Green, R.L. Kisliuk and F.T. Lin, *Bioorg. Med. Chem.*, **13**, 5475 (2005).
3. S.K. Kim, Z.G. Gao, L.S. Jeong and K.A. Jacobson, *J. Mol. Graph. Model.*, **25**, 562 (2006).
4. C.H.T.P da Silva, V.L. Campo, I. Carvalho and C.A. Taft, *J. Mol. Graph. Model.*, **25**, 169 (2006).
5. Q. Deng, Z. Lu, J. Bohn, K.P. Ellsworth, R.W. Myers, W.M. Geissler, G. Harris, C.A. Willoughby, K. Chapman, B. Mckeever and R. Mosley, *J. Mol. Graph. Model.*, **23**, 457 (2005).
6. D.A. Gschwend, W. Sirawaraporn, D.V. Santi and I.D. Kuntz, *Science*, **259**, 1445 (1998).
7. M.V. Teijido, I. Caracelli and J. Zukerman-Schpector, *J. Mol. Graph. Model.*, **24**, 349 (2006).
8. M. Martic, I. Tatic, S. Markovic, N. Kujundzic and S. Kostrun, *Eur. J. Med. Chem.*, **39**, 141 (2004).
9. B. Roth, *Fed. Proc.*, **45**, 2765 (1986).
10. J. Jolivet, K.H. Cowan, G.A. Curt, N.J. Clendenin and B.A. Chabner, *N. Eng. J. Med.*, **309**, 1094 (1983).

11. J.R. Bertino, E. Goker, R. Gorlick, W.W. Li and D. Banerjee, *Stem Cells*, **14**, 5 (1996).
12. J. Davoll and A.M. Jhonson, *J. Chem. Soc.*, 997 (1970).
13. E. Bolsch, E. Gralla and J.R. Bertino, *Ann. N.Y. Acad. Sci.*, **486**, 501 (1976).
14. D.J. Hutchson, *Cancer Chemother. Rep.*, **52**, 1 (1968).
15. M. Shimoyama and D. Hutchson, *Proc. Am. Assoc. Cancer Res.*, **10**, 80 (1969).
16. J.B. Hynes, J.M.Buck, L. D'souza and J.H. Freishem, *J. Med. Chem.*, **18**, 1191 (1975).
17. C. Hansch, J.Y. Fukunaga, P.Y.C. Jow and J.B. Hynes, *J. Med. Chem.*, **20**, 96 (1977).
18. W.I. Cowell, V.H. Brown, J.I. Degraw and N.I. Morrison, *Dev Biochem.*, **4**, (1978); *Chem. Abstr.*, **91**, 69172d (1979).
19. S.J. Yan, L.T. Weinstock and C.C. Cheng, *J. Heterocycl. Chem.*, **16**, 541 (1979).
20. Glide 4.0 User Manual, Schrodinger Press, Schrodinger Co. Ltd., USA.
21. H.D. Holtje, W. Sippl, D. Rognan and G. Folker, Molecular Modeling-Basic Principles and Applications, Wiley-VCH Gmbh & Co., Germany, edn. 2, p. 155 (2003).
22. L. Yamini and M. Vijjulatha, *E-J. Chem.*, **5**, 263 (2008).
23. QikProp 2.5 User Manual, Schrodinger Press, Schrodinger Co. Ltd., USA.

(*Received*: 29 August 2008; *Accepted*: 30 April 2009) AJC-7478